1997 JANNAF Propulsion Systems Hazards Subcommittee Meeting, West Palm Beach, FL (27-31 Oct 97)

Millisecond Burning of Confined Energetic Materials During Cookoff*

R.G. Schmitt and T.A. Baer

Sandia National Laboratories, Albuquerque, New Mexico 87185†

ABSTRACT

To predict the violence of reaction of confined energetic materials during cookoff requires a description of the relevant physical processes that occur on time scales ranging from days to submicroseconds. The time-to-ignition can be characterized accurately using heat transfer with chemistry and quasi-static mechanics. After ignition the energetic material deflagrates on a millisecond time scale. During this time the mechanical processes become dynamic. If the confinement survives burning then accelerated deflagration can lead to shock formation and deflagration to detonation transition. The focus of this work is the dynamic combustion regime in the millisecond time domain. Due to the mathematical stiffness of the chemistry equations and the prohibitively fine spatial resolution requirements needed to resolve the structure of the flame, an interface tracking approach is used to propagate the burn front. Demonstrative calculations are presented that illustrate the dynamic interaction of the deflagrating energetic material with its confinement.

INTRODUCTION

The response of a system containing an energetic material (EM) to an abnormal thermal environment is termed "cookoff." The environment may be a severe condition, such as a fuel-fire, or a slow process of heat addition in which the temperature increases a few degrees per hour. This response of the EM system to the thermal environment can vary from an essentially quiescent pressure burst to a very violent detonation-like event. To predict this response requires analysis of time scales ranging from hours to submicroseconds, see Fig. 1. The initial phase of the analysis is represented by heat conduction with chemistry and quasi-static mechanics [1]. During this phase of the analysis the time-to-ignition is determined and the state of the EM may also be characterized. The mechanical state of the energetic material is derived from a constitutive mechanics model [2,3]. The constitutive model must be capable of describing the response of the energetic material to mechanical loading, thermal expansion, chemical decomposition and damage. A validated constitutive model that accounts for these effects has yet to be developed. At ignition the EM begins to burn in a millisecond regime at rates varying from 1 to 1000's of centimeters per second. Also, the mechanical response of the system becomes dynamic. A dynamic constitutive model for the energetic material must now describe the stress rate as a function of the strain rate and damage state. The damage state may be characterized by porosity, specific surface area, and crack density. The confinement dynamics determine the response of the system. If the confinement fails during burning, a less violent event ensues. However, when the confinement survives the initial stages of burning, then accelerated combustion leads to shock formation and favors a violent deflagration to detonation transition (DDT) event [4]. Shock physics analysis is then required to predict the subsequent level of violence. The focus of this paper is on the millisecond burn regime with dynamic mechanics.

ANALYSIS

One approach to describing the dynamic combustion regime during cookoff is to resolve the flame structure of the burning EM [5]. (An idealized flame structure for a nitramine, such as undamaged HMX, is shown in Fig. 2.) There is a fizz zone adjacent to the burning surface, followed by an induction or dark zone, and a secondary flame zone [6]. Notice that the condensed-phase chemistry is confined to a thin layer just below the burning surface and throughout the fizz zone. The secondary flame is primarily com-

*Approved for public release; distribution is unlimited

†This work performed at Sandia National Laboratories supported by the U.S. Department of Energy under contract DE-ACO4-94AL85000.

DISCLAIMER

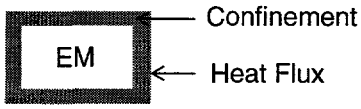

Interaction with confinement determines the level of violence

Heat conduction and chemistry coupled to quasi-static mechanics	Dynamic mechanics with burn propagation	Determine DDT
Preignition heat addition	Postignition deflagration	Shock physics analysis
hours minutes seconds	milliseconds	microseconds

Figure 1. Confined energetic material in an abnormal thermal environment with the appropriate physics prescribed at the appropriate time scale.

posed of gas-phase chemistry which is highly pressure dependent. A simplified set of equations that describe this structure include multi-step chemistry and conductive heat transfer. At the conditions encountered in cookoff (i.e., high pressure) the dark zone collapses and the flame structure is reduced to the order of a few micrometers [6]. At these conditions the multi-step chemistry equations become mathematically stiff. To accurately represent the physics of the flame propagation requires the resolution of the flame structure. The necessary spatial resolution is prohibitive (even in one dimension with adaptive gridding) and the stiff chemistry severely reduces the time step. The flame structure for a damaged EM is similar but contains the multiphase, multicomponent effects of gas permeation into the unburned material and convective transport [7,8]. Clearly, resolving the flame structure is not feasible, especially in multidimensional simulations, and an alternative approach is required.

The approach taken here to eliminate the time step and spatial resolution restrictions is to replace the flame structure by a mathematical discontinuity. The discontinuity or flamesheet is represented by jump conditions across the flame structure and requires the specification of a flame velocity. An interface tracking method is used to locate and propagate the burn front discontinuity when required. For illustration, consider the unstructured finite element mesh shown in Fig. 3. The scalar volume fraction field of the reacted material is represented by the number contained in each element. At some point in the calculation, it is necessary to determine the orientation and location of the burn front discontinuity. The orientation is determined by using the volume fraction of the materials in the elements surrounding the burn front to compute a local volume fraction gradient which is normal to the burn front. The burn front is then located by constructing an interface with this normal that matches the element volume fraction. This is a standard volume of fluid approach extended to unstructured finite element meshes [9,10]. The reconstructed interface can then be propagated in response to the local condi-

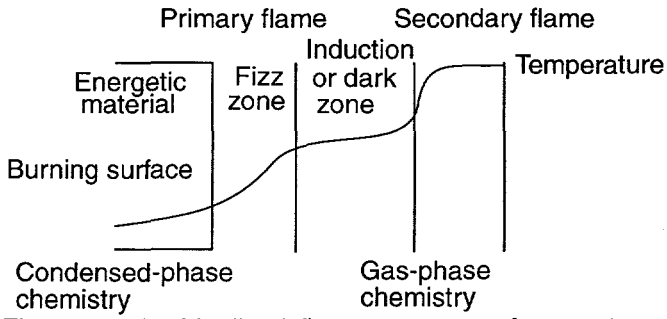

Figure 2. An idealized flame structure of an undamaged nitramine, such as HMX.

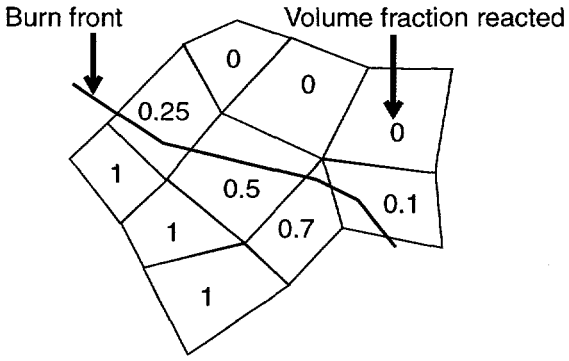

Figure 3. An unstructured finite element mesh illustrating the methodology for determining the orientation and location of a burn interface.

tions (pressure, temperature and specific surface area). The interface propagation is represented by the solution to an advection equation:

$$\frac{\partial F}{\partial t} + V_m \nabla F - V_F |\nabla F| = 0 \tag{1}$$

where F(X,t) represents the flame surface, V_m is the local material velocity, and V_f is the flame velocity relative to the unreacted material. The solution to this equation is very complicated for multimaterial elements on unstructured meshes and is solved algorithmically for efficiency. That is, the orientation and location of the interface along with the propagation velocity determine when the interface moves into adjacent elements. This analysis also requires the specification of the flame velocity. A simple empirical expression, such as $V_f = aP^n$, could be used to represent the flame velocity of an undamaged energetic material. However, the combined thermal/chemical and mechanical insults suffered by confined energetic materials create damage states with enhanced surface area that require further analysis [7]. For the present study the flame velocity is represented by the functional form given in Eq. (2) with separate generic functions representing the pressure, temperature and specific surface area dependencies:

$$V_F = F_1(P,\lambda)F_2(T,\lambda)F_3(A,\lambda) \tag{2}$$

where λ is an extent of reaction progress variable that can also be used to determine the propagation velocity. For the present paper the burn velocity functions are: $F_1 = aP^n$, $F_2 = (T/To)^\sigma$, and $F_3 = 1+\beta\lambda$. Note that F_3 represents an enhancement to the specific surface area caused by chemical decomposition. In the future the combustion physics of the burn front will be incorporated into the propagation using an embedded asymptotic analysis of the deflagration of porous energetic materials to specify the flame velocity [8]. This burn model has been incorporated into ALEGRA, an arbitrary Lagrangian-Eulerian finite element analysis program developed at Sandia National Laboratories [11].

The unstructured finite element mesh shown in Fig.4 was used to test the burn model propagation scheme. This geometry was modeled with rigid walls and a constant velocity burn was initiated from the center of the box. Also shown in Fig. 4 are three time planes from the burn propagation which demonstrate that the burn model adequately propagates a circular burn. The burn model can now be used to study the dynamics of the interaction between the burning EM and its confinement. Several demonstrative calculations are presented illustrating this dynamic interaction. A key feature of this implementation is that the burn front propagation is independent of the constitutive models that are used for EM and its product gas. Therefore, many different constitutive models can be used or interchanged as the problem physics dictate.

RESULTS AND DISCUSSION

A series of calculations are presented that demonstrate the capabilities of the burn model. For these simulations the thermochemical properties of HMX are used for the EM. The first set of calculations was performed on the TNO-PML cookoff configuration shown in Fig. 5 [12]. This is a cylindrical pipe with large endcaps that is heated with an electrical resistance wire from the sides. This configuration has been outfitted with a series of diagnostics including thermocouples, pressure gauges, and strain gauges. A fast cookoff thermal/chemical analysis was performed using the finite-element analysis code COYOTE [13]. Experimental observations suggest that fast cookoff results in a less violent event due to the loss of confinement early in the burning process. The surface temperature of the cylinder was ramped at 9.5 K per minute until ignition, at approximately 1500 s. Also shown in Fig. 5 are the temperature and the extent of reaction (λ) contours just prior to ignition. Notice that ignition occurs next to the inner surface of the cylinder in the center and that the decomposition is confined to a small layer next to the inner wall of the cylinder. The burn propagation is anticipated to propagate more rapidly along the inner surface due to its greater extent of decomposition. A coupled thermal/chemical and mechanical analysis of this configuration could also be performed [1]. However, for purposes of demonstration, the thermal/chemical analysis is used as an initial condition for the burn propagation. A simple linear elastic representation is used for the dynamic EM constitutive model. This is recognized as a vast simplification to the actual mechanical

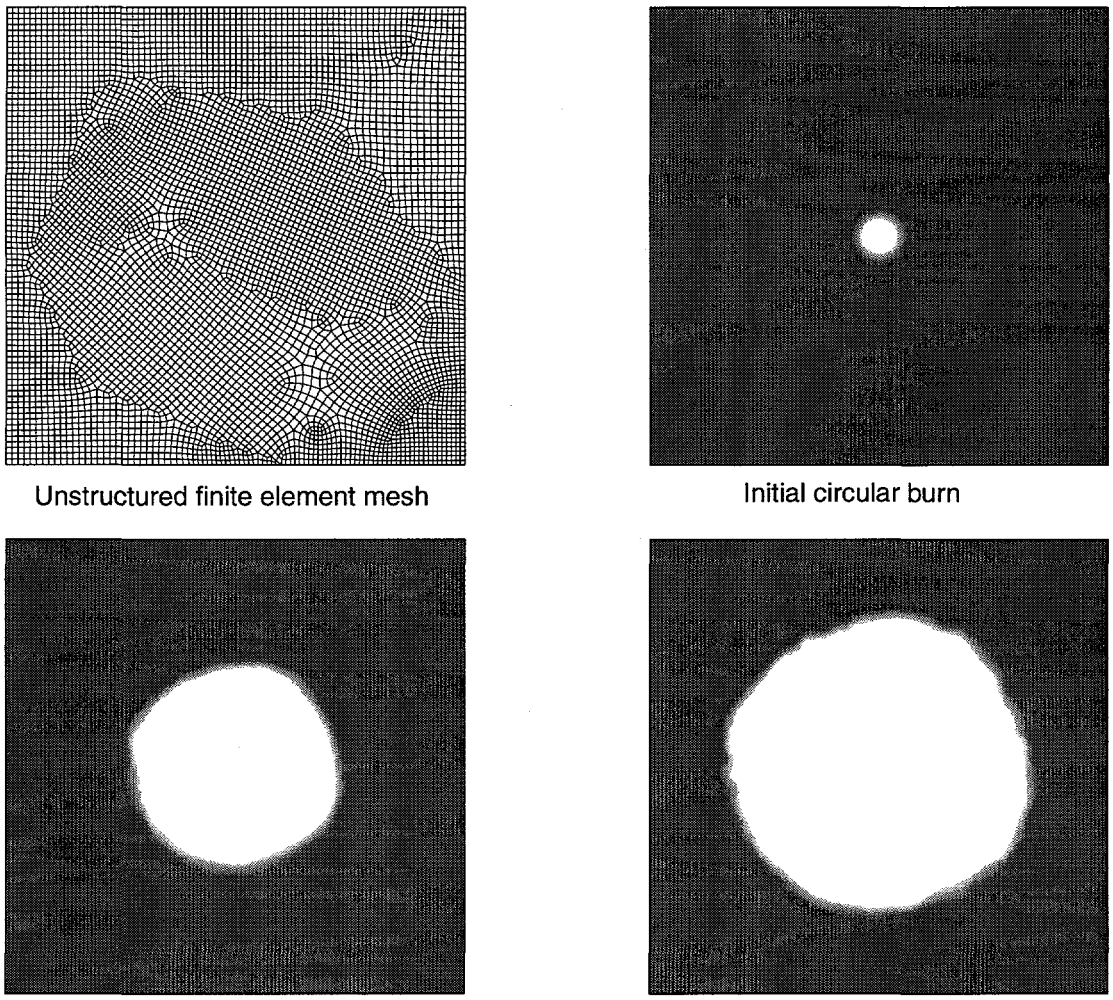

Figure 4. Burn propagation test problem with the unstructured finite element mesh (upper left) and the initial circular burn (upper right). The burn propagation is shown after 0.5 and 1.0 ms.

response of confined EM's [2,3,14] which may be characterized by an elastic-plastic, viscoelastic, visco-plastic response with damage and modifications due to chemical composition and compaction.

The first stage of the postignition burn simulation is transferring the temperature and extent of reaction fields from the thermal/chemical analysis into the burn computational mesh. Presently, these are stored as internal state variables for each element and are used in Eq. (2) to calculate the burn velocity. In the future, the calculation will be initialized from a coupled thermal/chemical and quasi-static mechanics analysis [1]. The burn is initialized by placing a small spherical bubble of reaction products at the location of ignition. The reaction products model is represented by the Noble-Abel equation of state [15]. The burn propagation, represented by a series of time-planes from the post ignition simulation, is shown in Fig. 6. Initially the burn front propagates at rates ranging from 1-25 cm/s and accelerates as the pressure increases. At approximately 0.72 ms, the burn velocity has reached slightly over 500 cm/s and the confinement fails. After the confinement fails, the burn product gas is vented and the reaction is quenched (i.e., burn velocity approaches zero). The burn has propagated approximately 5 times faster in the axial direction than in the radial. This propagation is a result of assuming that the extent of reaction variable is

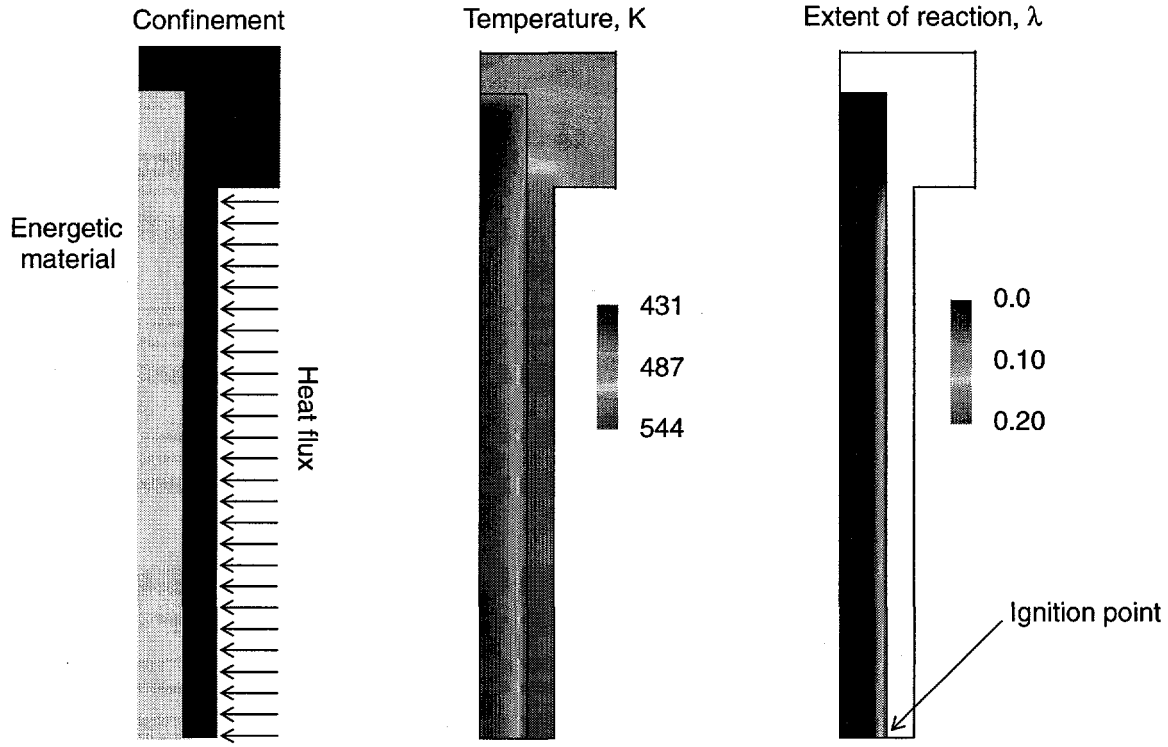

Figure 5. Thermal chemical analysis of the TNO-PML cookoff configuration shown on the left where an energetic material is confined in a cylindrical geometry. For this simulation the heat flux applied at the outer wall causes a linear increase in temperature at 9.5 K per minute. The temperature and extent of reaction contours are shown at 1500 seconds just prior to ignition.

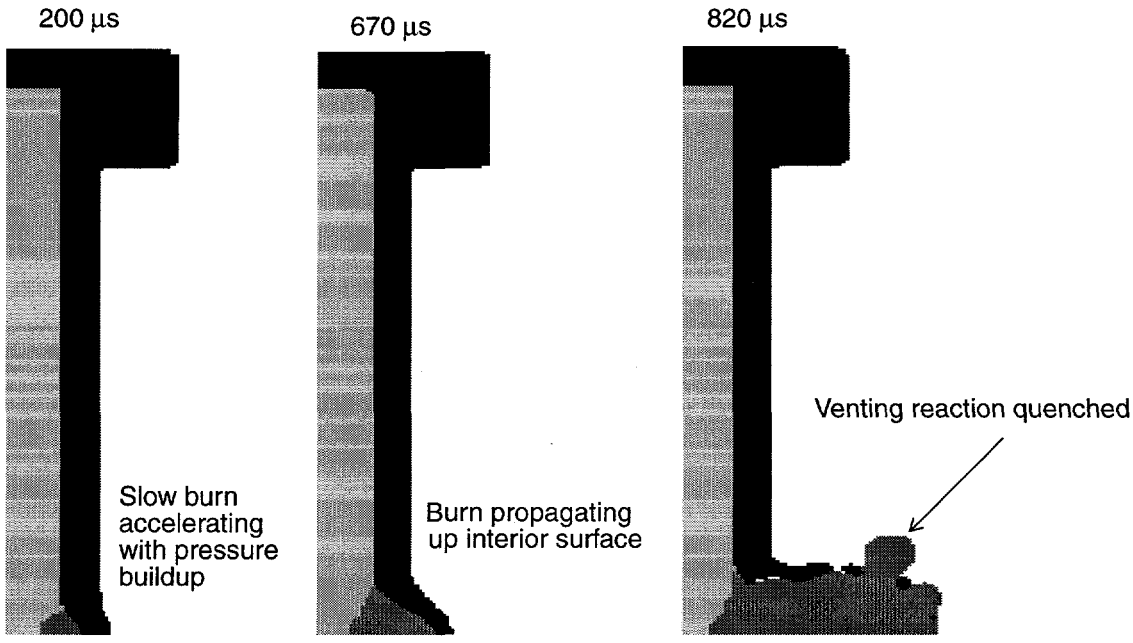

Figure 6. Postignition deflagration of the TNO-PML fast cookoff test at 200, 670 and 820 μs after ignition showing the burn propagation after thermal/chemical analysis indicated ignition occurred near the outer wall.

related to a porous damage state of the energetic material and can be used as a burn modifier [7]. The simulation used a simple yield stress dependent fracture model to break and fragment the confinement [16]. In the future, strain rate calculations of the confining materials can be used to estimate the amount and characteristic dimension of the fragments caused by the burning process [4]. This calculation demonstrates qualitatively the burning behavior of the EM during fast cookoff.

The thermal/chemical analysis of slow cookoff for the TNO-PML configuration, not shown due to space limitations, predicts that ignition occurs in the center of the EM with a more uniform temperature and extent of reaction contours. Simulation of the postignition combustion events and confinement dynamics is shown in Fig. 7. For the slow cookoff burn simulation, a spherical bubble of product gas is inserted in the center of the EM. The slow cookoff thermal chemical analysis predicts that a small core of reacted material exists in the center of the EM. Similar to the fast cookoff simulation, this core is used as a burn modifier to enhance the burn rate. At 160 μs the burn has spread rapidly up the centerline. As suggested by the time scale of confinement failure (200 μs), the qualitative degree of damage to the TNO-PML pipe, and the greater mass of EM consumed, the slow cookoff case would yield a more violent reaction than the fast cookoff case.

To complete the demonstrative calculations, a fully three-dimensional simulation of the Naval Surface Warfare Center variable confinement cookoff test (VCCT) is presented [17]. The VCCT configuration is shown in Fig. 8, where two relatively heavy end plates are bolted together to provide confinement for an EM that is contained in an aluminum sleeve, variable thickness steel sleeve, and a heater band (which extends approximately 80% around the circumference of the steel sleeve) and is used to provide heating. The configuration must be analyzed in three dimensions due to the bolts that provide confinement. Note also that there is a symmetry plane at 180 degrees due to the current orientation of the heater band. However, for generality this symmetry plane was not used.

The results obtained from the experimental test are thermocouple traces and a qualitative categorization of the violence of the event [18]. That is, the number of fragments produced are subjectively related to the violence of reaction. Current computational models for fracture and fragmentation are empirical and will not be able to calculate fragmentation explicitly. In the future, Grady-Kipp [19] fragmentation theory will be used with calculated strain rates to estimate the confinement fragmentation and its relationship to the experimental conditions and violence categorization.

A previous quasi-static and thermal/chemical analysis of the VCCT predicted that ignition occurs in the center of the EM with a nearly uniform temperature field [4]. The analysis of the postignition combustion events demonstrated the capability to predict the high-order responses from explosions to DDT. The current burn dynamics propagation model extends this capability to predictions ranging from pressure burst to explosions. The first stage of the VCCT analysis is to perform scoping calculations of the confinement dynamics with the burn propagation to determine computational expense, meshing requirements and model parameters. For this set of calculations, a 2D horizontal cross section at the height of the heater band is used. The burn is initiated centrally by inserting a small spherical bubble of product gas. The 2D simulation uses the arbitrary Lagrangian-Eulerian (ALE) capabilities of ALEGRA. The EM finite element block is chosen as Eulerian with a Lagrangian slide surface at the interface with the aluminum sleeve. The aluminum sleeve, steel sleeve and heater band blocks are ALE with slide surfaces at the material interfaces. This arrangement is shown in Fig. 9 along with two time planes from the burn propagation simulation. Note that due to the Lagrangian nature of the interfaces between element blocks, fracture, fragmentation and mixing of the materials is not permitted. The simulation is terminated when deformation is too large to resolve in a Lagrangian (or ALE) fashion. The significant deformation to notice in the mesh shown in Fig. 9 is located at the boundary between the EM and the aluminum sleeve. The ALE mesh is shown at 40 and 140 μs and a representation of the burn front location is also given. At 140 μs, the heater band has slid significantly along the outer surface of the steel sleeve. This implies that for the 3D Eulerian simulation, the heater band does not provide much confinement. The 2D simulation also yields a good estimate for the time to confinement failure at approximately 160 μs. For later reference, the 2D simulations were performed on Sun workstations in a few hours.

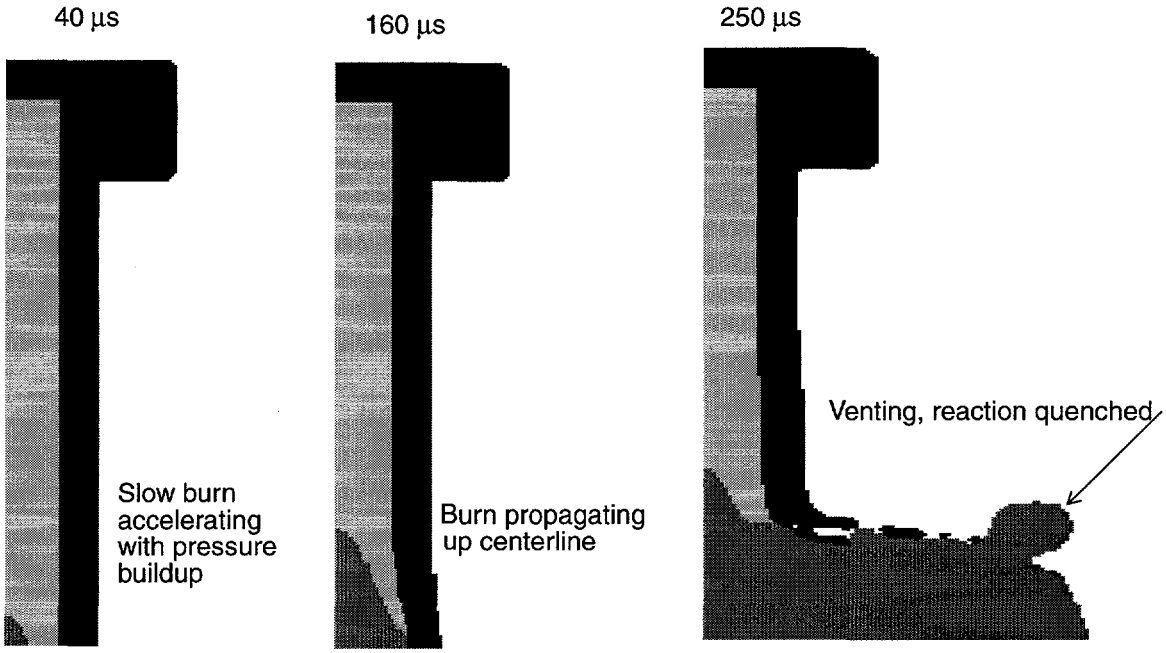

Figure 7. Postignition deflagration of the TNO-PML cookoff test at 40, 160, and 250 μs after ignition. Burn was initiated in the center of the EM and propagated rapidly up the centerline.

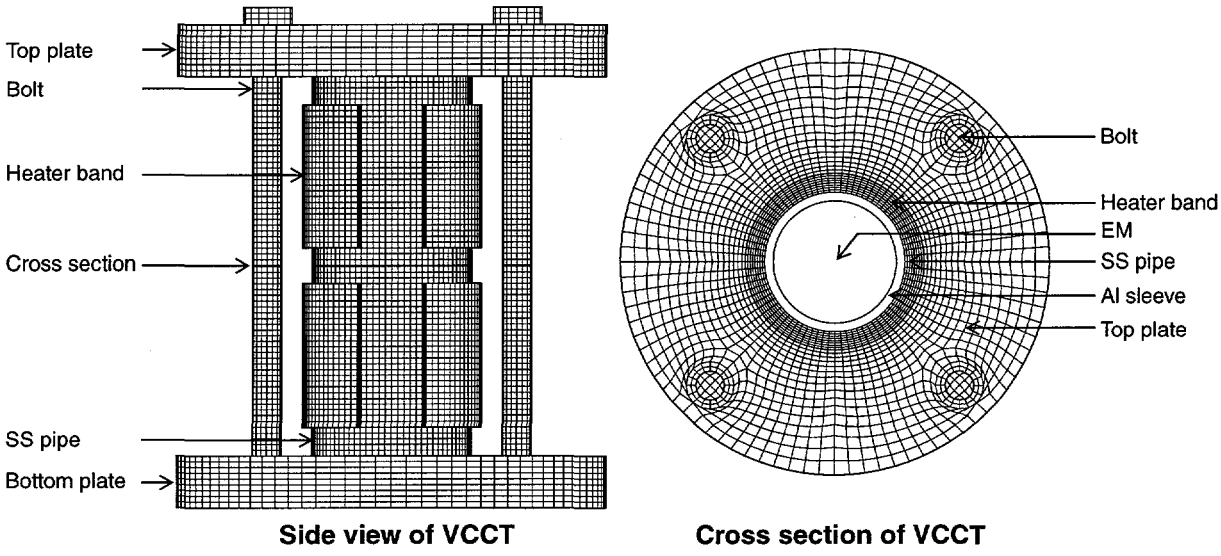

Figure 8. Finite element computational mesh of the variable confinement cookoff test (VCCT). The mesh contains 207,000 elements and is a full three-dimensional representation of the hardware.

Three time planes from the 3D simulation of the burn propagation in the VCCT geometry are shown in Fig. 10. The 3D simulation was conducted using an Eulerian description of the geometry. This has several implications on the dynamics of the confinement. For Eulerian calculations, the material interfaces do not slide relative to each other which effectively means they are welded together. This is not acceptable for the heater band due to the gap around the circumference. The heater band in 3D is allowed to fracture to allow a more realistic representation of its behavior. At 50 μs, the burn has only propagated a short distance and there is no significant deformation of the confinement. At 154 μs, the burn has propagated to the interior of the confinement and the product gases have started to vent. There is significant fracture and deformation of the confinement. Similarly, at 218 μs, the confinement has fragmented into several large pieces while continued venting quenches the burn front propagation. The burn velocity was approximately 10 cm/s initially and accelerated to over 2000 cm/s as the internal pressure increased. These are realistic velocities for the anticipated burn rates [20,21]. The full 3D simulations are computationally expensive. If performed on the same workstation as the 2D simulations these calculations would take several weeks to complete. The Teraflop computer located at Sandia National Laboratories in Albuquerque, New Mexico allows these calculations to be performed in under a day [22].

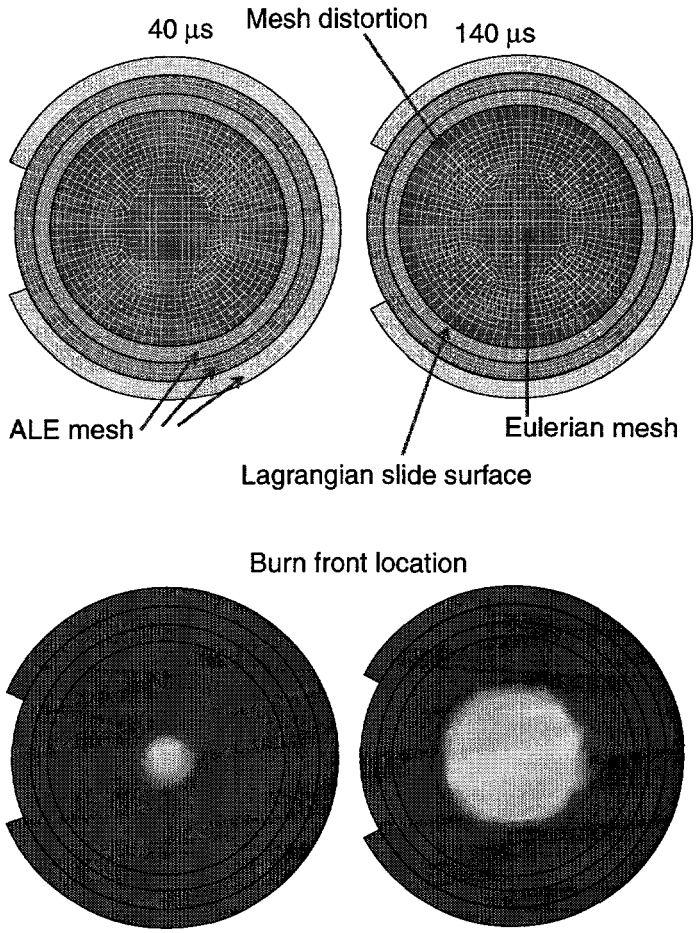

Figure 9. Two-dimensional simulation of a cross section of the VCCT with slide lines between material interfaces: the top shows the ALE mesh configuration while the bottom shows burn front location.

It should be noted that the burn propagation is significantly different from the traditional method of programmed detonation. A programmed detonation propagates a reaction front at a specified velocity and produces specified thermodynamic expansion states. Here, the burn front propagates in response to local conditions (pressure, temperature, material state) and is also advected with the material velocity. This is part of the reason for the nonsymmetric appearance of the burn front, see Fig. 9. Another reason for the nonsymmetric propagation is attributed to the method for determining the orientation and propagation of the burn front. Under certain circumstances, this method can misorient interfaces causing mesh-biased propagation. Several techniques are being investigated for reducing mesh-biased results including mesh adaptivity, finer resolution meshes, using ALE capabilities, and improvements to the existing propagation algorithm to recognize biased meshes. It should be mentioned that the material velocity is also biased by mesh orientation which adversely affects the symmetry of the burn front.

SUMMARY AND CONCLUSIONS

A burn model has been developed to describe the millisecond dynamic combustion regime for confined EM's. This model allows the determination of the dynamic interaction of the confinement to the combustion behavior of damaged EM's. This is a necessary step toward predicting the violence of reac-

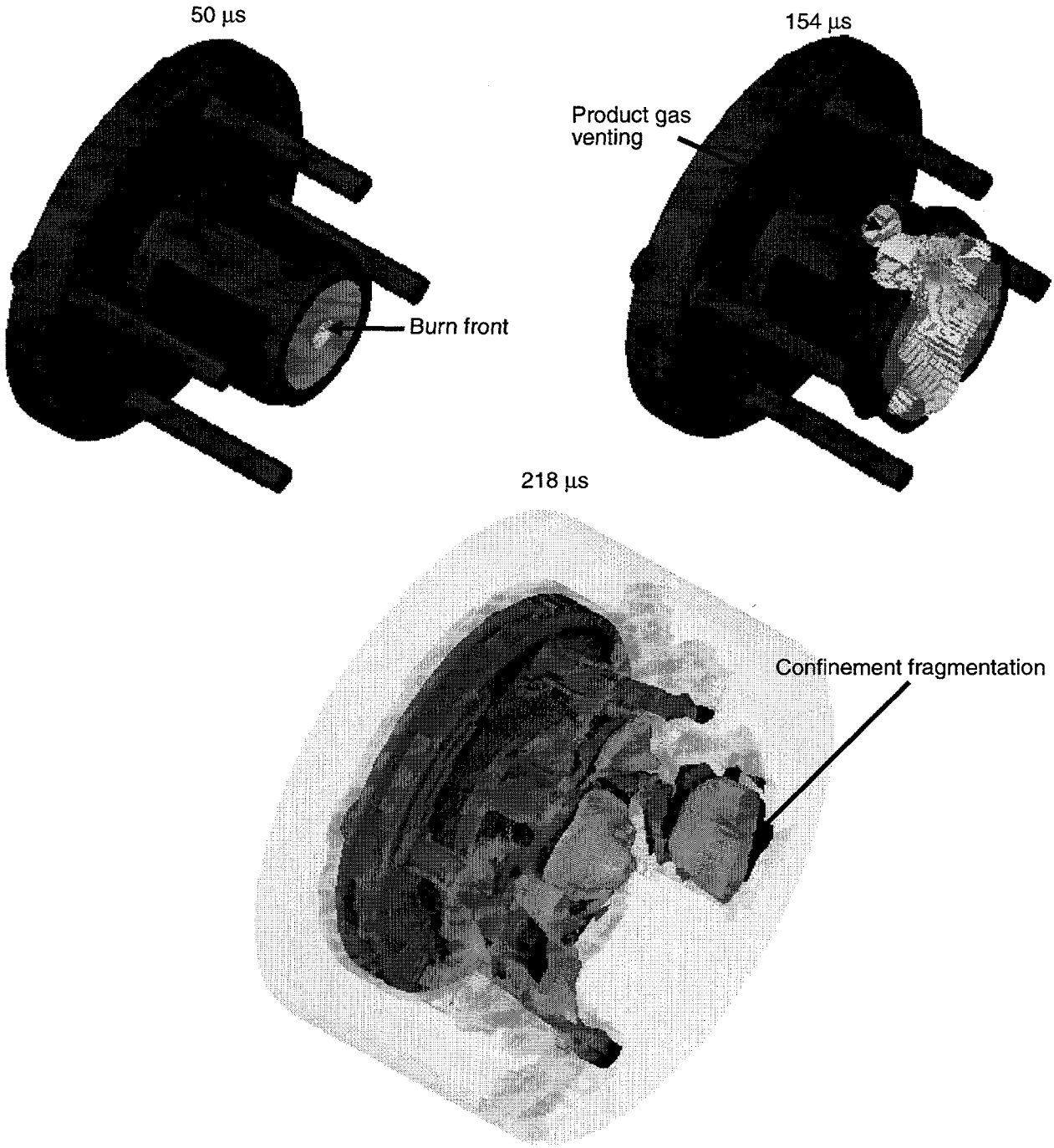

Figure 10. Postignition deflagration in the VCCT slow cookoff test at 50, 154 and 218 µs after ignition showing burn propagation, product gas venting and confinement fragmentation. Burn was initiated in the center of the EM as calculated by thermal/chemical analysis.

tion. A series of calculations demonstrated the behavior of the burn model. The future direction of the model development involves introducing more of the appropriate combustion physics into the burn propagation using asymptotic analysis techniques. Also, methods for decreasing mesh-biased propagation are being investigated. The development and validation of mechanical constitutive models applicable to thermally degraded EM's with chemical composition changes in the quasi-static and dynamic regimes is a necessary step for realistic simulations of confined EM's during cookoff. Similarly, the development of fracture and fragmentation models for the confining materials under the conditions encountered in cookoff is also an important need for the development of predictive capability for cookoff violence. The burn model presented here represents one class of burning that is expected in cookoff. The development of other burn models (e.g., convective combustion fronts) is required to model granulated EM's, such as gun propellants, during cookoff. Finally, to validate the burning behavior of this model requires experimental measurements of the burn rates of degraded and damaged EM's.

ACKNOWLEDGMENT

We would like to express our appreciation to Mike Hobbs and Mike Glass for their help with the visualization of the computational results.

REFERENCES

1. M. L. Hobbs, M. R. Baer and R. J. Gross, "Thermal-Chemical-Mechanical Cookoff Modeling," *JANNAF Propulsion Systems Hazards Subcommittee Meeting*, CPIA Publication 615, San Diego, CA, 311, 1994.
2. A. M. Renlund, J. C. Miller, and K. L. Erickson, "Characterization of Energetic Material Response to Thermal Environments," *1996 JANNAF Propulsion Systems Hazards Subcommittee Meeting, Naval Postgraduate School,* Monterey, CA, 1996.
3. M. L. Hobbs, R. G. Schmitt and A. M. Renlund, "Analysis of Thermally-Degrading, Confined HMX," *1996 JANNAF Propulsion Systems Hazards Subcommittee Meeting*, Naval Postgraduate School, Monterey, CA, 1996.
4. M. R. Baer, M. E. Kipp, M. L. Hobbs, and R. G. Schmitt, "Toward Assessing the Violence of Reaction During Cookoff of Confined Energetic Materials," *1996 JANNAF Propulsion Systems Hazards Subcommittee Meeting,* Naval Postgraduate School, Monterey, CA,1996.
5. E. S. Oran and J. P. Boris, Numerical Simulation of Reactive Flow, Elsevier Science Publishing Co., Inc., New York, New York, 1987.
6. T. L. Boggs, "The Thermal Behavior of Cyclotrimethylenetrinitramine (RDX) and Cyclotetramethylenetetranitramine (HMX)," Chapter 2, Fundamentals of Solid Propellant Combustion, Progress in Astronautics and Aeronautics, (K.K. Kuo and M. Summerfield, Eds.), Vol. 90, pp.121-175, 1984.
7. S. B. Margolis and F. A. Williams, "Effects of Two-Phase Flow on the Deflagration of Porous Energetic Materials," J. Propulsion and Power, Vol. 11, pp. 759-768, 1995.
8. S. B. Margolis, "Influence of Pressure-Driven Gas Permeation on the Quasi-Steady Burning of Porous Energetic Materials," SAND97-8688, Sandia National Laboratories, Livermore, September, 1997.
9. C. W. Hirt and B. D. Nichols, "Volume of Fluid (VOF) Method for the Dynamics of Free Boundaries," Journal of Computational Physics, Vol. 39, pp. 201-225, 1981.
10. N. Ashgritz and J. Y. Poo, "FLAIR: Flux Line-Segment Model for Advection and Interface Reconstruction," Journal of Computational Physics, Vol. 93, pp. 449-468, 1991.
11. R. M. Summers, J. S. Peery, M. K. Wong, E. S. Hertel, T. G. Trucano, and L. C. Chhabildas, "Recent progress in ALEGRA development and application to ballistic impacts," SAND96-0045C, Sandia National Laboratories, Albuquerque, NM, 1996.
12. J. H. G. Scholtes, B. J. van der Meer, "Temperature and strain gauge measurements in the TNO-PML Cook-off test," TNO report PML 1996-A62, 1997.
13. D. K. Gartling and R. E. Hogan, "COYOTE II- A Finite Element Computer Program for Nonlinear Heat Conduction Problems," SAND94-1173, Sandia National Laboratories, Albuquerque, NM, 1994.
14. M. P. Brubernak, et. al., "Propellant Hazard Test and Analysis Program," Final Report- Year 3, LMSC/9418124, Lockheed Martin Missiles & Space, Sunnyvale, CA, March, 1995.
15. R. G. Schmitt, P. B. Butler and N. French, "Chemkin Real Gas: A Fortran Package for Analysis of Thermodynamic Properties and Chemical Kinetics in Nonideal Systems," University of Iowa Rpt. UIME-PBB-006, December 1993.
16. J. M. McGlaun, S. L. Thompson, and M. G. Elrick, "CTH: A Three-Dimensional Shock Physics Code," Int. J. Impact Engng, Vol. 10, pp. 351-360, 1990.

17. K. Alexander and K. Gibson, "Variable Confinement Cookoff Test," Naval Surface Warfare Center, Indian Head Division, White Oak Detachment, Memorandum dated November 7, 1994.

18. K. Gibson, "Variable Confinement Cookoff Test (VCCT) Results (Aug90-Nov91)," Naval Surface Warfare Center, Indian Head Division, White Oak Detachment, Memorandum dated December 6, 1991.

19. M. E. Kipp, D. E. Grady, and J. W. Swegle, "Numerical and Experimental Studies of High-Velocity Impact Fragmentation," Int. J. Impact Engng, Vol. 14, pp. 427-438, 1993.

20. A. F. Belyaev, V. K. Boblev, A. I. Korotkov, A. A. Sulimov, and S. V.Chuiko, Transition from Deflagration to Detonation in Condensed Phases, Translated from Russian, Israel Program for Scientific Translations, 1975.

21. H. H. Bradley and T. L Boggs, "Convective Burning in Propellant Defects: A Literature Review," China Lake, CA, Naval Weapons Center, Feb. 1978.

22. T. G. Mattson, S. Scott, and S. R. Wheat, "A TeraFLOP Supercomputer in 1996: the ASCI TFLOPS System," Proceedings of the International Parallel Processing Symposium, 1996.